

See discussions, stats, and author profiles for this publication at: <https://www.researchgate.net/publication/257951627>

# Symmetry-breaking diffraction and dynamic self-trapping in optically induced hexagonal photonic lattices

Article in *Applied Physics Letters* · February 2012

DOI: 10.1063/1.3682510

CITATIONS

5

READS

100

9 authors, including:



**Sheng Liu**

Northwestern Polytechnical University

90 PUBLICATIONS 1,116 CITATIONS

[SEE PROFILE](#)



**Yi Hu**

105 PUBLICATIONS 1,436 CITATIONS

[SEE PROFILE](#)



**Peng Zhang**

University of California, Berkeley

134 PUBLICATIONS 2,332 CITATIONS

[SEE PROFILE](#)



**Xuetao Gan**

Columbia University

111 PUBLICATIONS 2,875 CITATIONS

[SEE PROFILE](#)

Some of the authors of this publication are also working on these related projects:



2-D materials and electronics [View project](#)



Femtosecond laser processing crystals and photoelectric detectors [View project](#)

## Symmetry-breaking diffraction and dynamic self-trapping in optically induced hexagonal photonic lattices

Sheng Liu, Yi Hu, Peng Zhang, Xuetao Gan, Cibo Lou et al.

Citation: *Appl. Phys. Lett.* **100**, 061907 (2012); doi: 10.1063/1.3682510

View online: <http://dx.doi.org/10.1063/1.3682510>

View Table of Contents: <http://apl.aip.org/resource/1/APPLAB/v100/i6>

Published by the [American Institute of Physics](#).

---

### Related Articles

Spectrally resolved detection of mixed acoustic vibrations by photorefractive interferometry  
*J. Appl. Phys.* **113**, 054502 (2013)

Experimental investigation of the visibility dependence in a nonlinear interferometer using parametric amplifiers  
*Appl. Phys. Lett.* **102**, 011130 (2013)

Propagation of femtosecond terawatt laser pulses in N<sub>2</sub> gas including higher-order Kerr effects  
*AIP Advances* **2**, 042190 (2012)

Coupled electromagnetic TE-TM wave propagation in a layer with Kerr nonlinearity  
*J. Math. Phys.* **53**, 123530 (2012)

Optical logic gates using coherent feedback  
*Appl. Phys. Lett.* **101**, 191113 (2012)

---

### Additional information on *Appl. Phys. Lett.*

Journal Homepage: <http://apl.aip.org/>


Journal Information: [http://apl.aip.org/about/about\\_the\\_journal](http://apl.aip.org/about/about_the_journal)

Top downloads: [http://apl.aip.org/features/most\\_downloaded](http://apl.aip.org/features/most_downloaded)

Information for Authors: <http://apl.aip.org/authors>

## ADVERTISEMENT

**JANIS** Does your research require low temperatures? Contact Janis today.  
Our engineers will assist you in choosing the best system for your application.



10 mK to 800 K      LHe/LN<sub>2</sub> Cryostats  
Cryocoolers      Magnet Systems  
Dilution Refrigerator Systems  
Micro-manipulated Probe Stations

[sales@janis.com](mailto:sales@janis.com)      [www.janis.com](http://www.janis.com)  
Click to view our product web page.

# Symmetry-breaking diffraction and dynamic self-trapping in optically induced hexagonal photonic lattices

Sheng Liu,<sup>1</sup> Yi Hu,<sup>2</sup> Peng Zhang,<sup>3</sup> Xuetao Gan,<sup>1</sup> Cibo Lou,<sup>2</sup> Daohong Song,<sup>2</sup> Jianlin Zhao,<sup>1,a)</sup> Jingjun Xu,<sup>2</sup> and Zhigang Chen<sup>2,3</sup>

<sup>1</sup>The Key Laboratory of Space Applied Physics and Chemistry, Ministry of Education and Shaanxi Key Laboratory of Optical Information Technology, School of Science, Northwestern Polytechnical University, Xi'an 710072, China

<sup>2</sup>The Key Laboratory of Weak-Light Nonlinear Photonics, Ministry of Education and TEDA Applied Physics School, Nankai University, Tianjin 300457, China

<sup>3</sup>Department of Physics and Astronomy, San Francisco State University, San Francisco, California 94132, USA

(Received 21 December 2011; accepted 18 January 2012; published online 8 February 2012)

We demonstrate both experimentally and numerically linear symmetry-breaking diffraction and nonlinear dynamic self-trapping of an optical beam in hexagonal photonic lattices. We show that a stripe multivortex beam undergoes asymmetric linear diffraction, but evolves into a moving self-trapped beam under a self-defocusing nonlinearity. Fine features of symmetry-breaking in diffraction of elliptical multivortex beams are also observed and discussed. © 2012 American Institute of Physics. [doi:10.1063/1.3682510]

Linear and nonlinear beam propagation and associated dynamics in photonic lattices have attracted substantial research interests in the past decade. The periodicity of the lattice structure breaks the rotational symmetry of the uniform medium, leading to abundant novel discrete light behaviors mediated by discrete diffraction,<sup>1,2</sup> refraction,<sup>2,3</sup> and nonlinear self-trapping.<sup>4-7</sup> The symmetries exhibited in these discrete optical phenomena are determined by both lattice structures and initial excitations. It has been demonstrated that the deformation of the lattice structures can break the inherent symmetry of the lattice, resulting in anisotropic discrete diffractions and nonlinear localized states.<sup>6,8</sup> Recently, the study of the discrete light behaviors has been performed in settings beyond the simple square lattices, including ionic-type,<sup>9</sup> hexagonal,<sup>10,11</sup> honeycomb,<sup>8,12-14</sup> Kagomé<sup>15</sup> and three-dimensional<sup>16,17</sup> photonic lattices. Hexagonal structures, as typical Bravais lattices, are widely used in photonic crystals and photonic crystal fibers due to their large photonic band gaps originated from the reduced symmetry.<sup>18</sup> In hexagonal and honeycomb photonic lattices with the sixfold symmetry, lattice solitons along with light tunneling, diffraction, and interband transitions have been studied.<sup>10-14</sup> Especially in honeycomb photonic lattices, symmetry-breaking and Dirac dynamics due to lattice deformation<sup>8</sup> or nonlinearity<sup>14</sup> have been studied. In this paper, we report on experimental and numerical study of linear symmetry-breaking diffraction and nonlinear self-trapping of a moving soliton stripe in an optically induced hexagonal photonic lattice. Our results provide an approach to control the flow of light over periodic photonic structures by employing symmetry-breaking dynamics.

The paraxial propagation of a monochromatic light beam  $\phi$  in a photonic lattice can be governed by the normalized nonlinear Schrödinger equation,

$$\partial\phi/\partial z - i\nabla_{\perp}^2\phi/2 = i\Delta n\phi, \quad (1)$$

where  $\phi$  denotes the complex amplitude of the optical field,  $\nabla_{\perp}^2 = \partial_{xx} + \partial_{yy}$ ,  $\Delta n = V_l + F(|\phi|^2)$  is the modulation of the refractive index,  $V_l$  is the periodic potential of the photonic lattice, and the function  $F(|\phi|^2)$  denotes the nonlinear refractive index change induced by light beam  $\phi$  itself. The dimensionless parameters ( $x, y, z, \Delta n$ ) are related to the physical parameters ( $x', y', z', \Delta n'$ ) by the expressions  $(x, y) = k_0(\Delta n_0 n)^{1/2}(x', y')$ ,  $z = k_0\Delta n_0 z'$ , and  $\Delta n = \Delta n'/\Delta n_0$ , where  $\Delta n_0$  is a normalization parameter for refractive index change,  $k_0$  is the wave number of the light in vacuum, and  $n$  is the index of the medium. For a hexagonal photonic lattice optically induced in a photorefractive medium with a saturable nonlinearity, the periodic optical potential created by a lattice-inducing intensity pattern  $I_l$  can be expressed by  $V_l = -(1 + I_l)^{-1}$ .<sup>7</sup> Here,  $I_l$  is in the form of three wave interference [as shown in Fig. 1(a)] and can be expressed as  $I_l = A|\sum_n \exp(i\mathbf{k}_n \cdot \mathbf{r})|^2/9$ , where  $\mathbf{k}_1 = 4\pi/3d\{1, 0\}$ ,  $\mathbf{k}_{2,3} = 2\pi/3d\{-1, \pm\sqrt{3}\}$ ,  $d$  is the lattice spacing, and  $A$  corresponds to the characteristic intensity determining the modulation depth of the induced lattice potential.

Dropping the nonlinear term in Eq. (1), the Bloch modes  $b(x, y)$  as well as the band structure  $\beta(k_x, k_y)$  supported by the hexagonal lattice can be solved in the form of  $\phi = b(x, y)\exp(i\beta z)$ , where  $\beta$  is the propagation constant,  $k_x$  and  $k_y$  are the transverse wave vectors. The calculated first three transmission bands are displayed in Fig. 1(b), and the Bloch mode at the high-symmetry  $M_1$  point [as marked in Fig. 1(b)] is depicted in Fig. 1(c). As expected, the Bloch mode at the  $M_1$  point represents a multivortex optical field with a singly charged vortex residing in the middle of three adjacent humps, exhibiting a threefold symmetry corresponding to the local band structure.<sup>10</sup> Figure 1(d) depicts the diffraction property along the  $\Gamma$ -M-X line [see the inset of Fig. 1(b)], where the top, middle, and bottom panels represent the curves of the transmission band, the corresponding

<sup>a)</sup>Author to whom correspondence should be addressed. Electronic mail: jlzhao@nwpu.edu.cn.

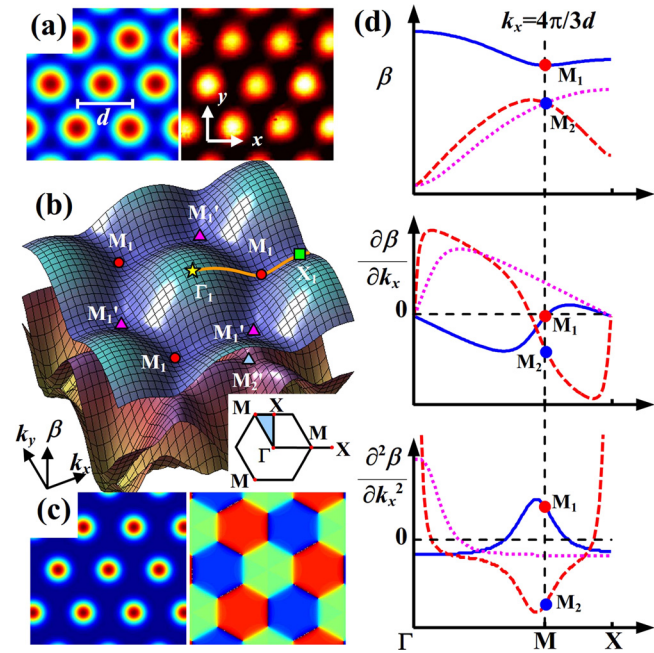


FIG. 1. (Color online) (a) Lattice structures in simulation (left) and experiment (right). (b) Transmission bands of the lattice with marked high-symmetry points. (c) Amplitude (left) and phase (right) of the Bloch mode at  $M_1$  point. (d) Band curve (top), refraction (middle), and diffraction (bottom) coefficients along the solid line in (b), where solid, dashed, and dotted lines correspond to the cases of first, second, and third band, respectively.

refraction ( $\partial\beta/\partial k_x$ ), and diffraction coefficient ( $\partial^2\beta/\partial k_x^2$ ), respectively. It can be seen that along the  $k_x$ -axis, the non-refraction ( $\partial\beta/\partial k_x=0$ )  $M_1$  point is located at the bottom of the 1st band within the anomalous diffraction region ( $\partial^2\beta/\partial k_x^2 > 0$ ). Interestingly, the diffraction around the  $M_1$  point is not symmetric, i.e., diffraction at the left-hand side of  $M_1$  is more intense than that at the right-hand side ( $|\partial^2\beta/\partial k_x^2|_{\text{left}} > |\partial^2\beta/\partial k_x^2|_{\text{right}}$ ). It is such asymmetric diffraction property that brings about peculiar linear and nonlinear beam dynamics. The  $M_2$  point is the crossing point of the 2nd and 3rd bands [see the top of Fig. 1(d)], around which the local diffraction coefficient also exhibits asymmetry. However, the asymmetry arisen from the strong mobility (positive refraction,  $\partial\beta/\partial k_x < 0$ ) of the  $M_2$ -point mode should be distinguished from the asymmetry diffraction property. Here, we shall only consider the non-refraction  $M_1$ -point mode.

To explore the asymmetric diffraction behavior at the  $M_1$  point, we first launch a quasi-one-dimensional multivortex beam [see Fig. 2(a)] into the hexagonal lattice, which is generated by truncating the Bloch mode at the  $M_1$  point with a stripe Gaussian envelope  $\exp(-x^2/4d^2)$ . As we can see from Fig. 2(b), the Fourier spectrum of the input beam is mainly distributed at  $\Gamma$ -M-X line, and different spectral components possess the different diffraction coefficients, as shown in the bottom of Fig. 1(d). Therefore, the linear diffraction will be governed by the asymmetric diffraction curve, i.e., those spatial frequency components residing between the  $\Gamma$  and M points refract toward right ( $\partial\beta/\partial k_x < 0$ ) and diffract intensely during propagation, while other components residing between the M and X points refract toward left ( $\partial\beta/\partial k_x > 0$ ) with much less diffraction.

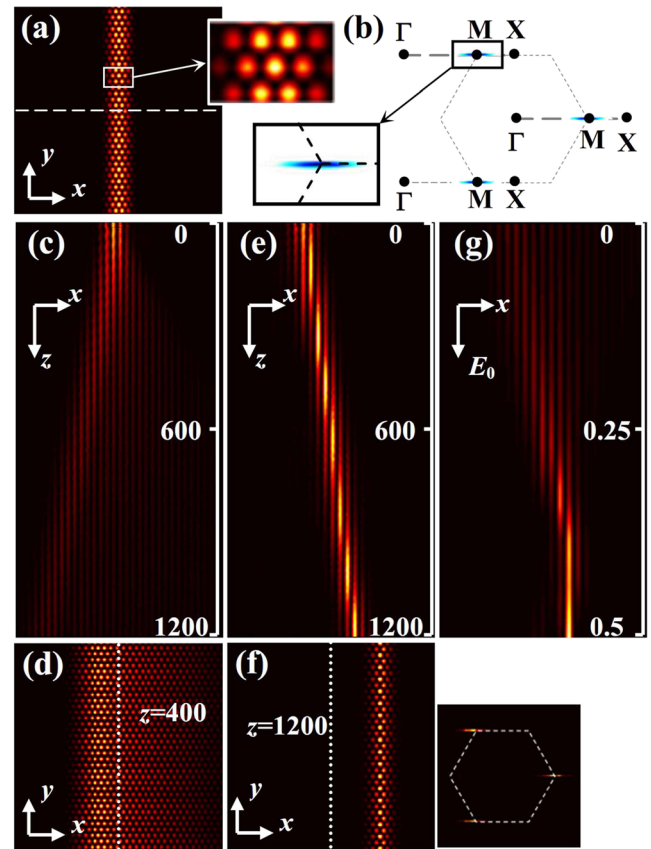


FIG. 2. (Color online) Numerical simulations on asymmetric linear diffraction and moving nonlinear self-trapping of a stripe multivortex beam. Input beam (a) and its Fourier spectrum (b), respectively, with the 1st Brillouin zone denoted by dashed hexagon. Side views of the linear (c) and nonlinear (e) beam propagations along  $z$ -direction for a section marked by the dashed line in (a). Linear (d) and nonlinear (f) outputs at  $z=400$  and  $1200$ , respectively, with the beam center of the input beam marked by vertical dotted line. Inset in (f) shows the output Fourier spectrum. (g) Output intensity versus  $E_0$ .

To visualize such diffraction feature, we numerically solve Eq. (1) by setting  $d=6$ ,  $A=2$ . The numerical results are shown in Figs. 2(c) and 2(d). It is obvious that the input beam indeed undergoes asymmetric diffraction with the position of the peak intensity moving toward negative  $x$ -axis, breaking the inversion symmetry of the Gaussian envelope of the input multivortex beam. It is worth mentioning that the input stripe beam should be set with a proper width. If the beam is too wide, the Fourier spectrum is too narrow, and the spectral components with asymmetric diffraction coefficient are too weak to result in appreciable mode-shifting. On the other hand, the beam should not be too narrow to ensure that the spectrum is totally located at the monotone region (the right of the peak) of the diffraction coefficient curve. Otherwise, the diffraction pattern will be cluttered.

Now let us look at the *nonlinear* propagation of the input stripe multivortex beam under the influence of the asymmetric diffraction. Nonlinear self-trapping of multivortex beams in hexagonal photonic lattices has been reported before but under a *self-focusing* nonlinearity.<sup>10</sup> Here, we employ a *self-defocusing* nonlinearity to balance the anomalous diffraction when the  $M_1$ -point Bloch modes are excited. The nonlinear index modulation induced by propagating beam is governed by  $F(|\phi|^2) = E_0/(1 + |\phi|^2)$ , where  $E_0$  determines the strength of the nonlinearity of the medium. With



the same input beam as depicted in Fig. 2(a) (the peak intensity is set as 0.1), the nonlinear evolution of the beam at  $E_0 = 0.35$  is numerically simulated as shown in Figs. 2(e) and 2(f). As expected, the diffraction of the input beam is indeed balanced by the self-defocusing nonlinearity, and the self-trapped beam remains its shape (envelope) and spectrum (always at three M points) even after long-distance propagation [e.g., at  $z = 1200$  as shown in Figs. 2(e) and 2(f)], indicating the possible existence of a moving soliton state. More surprisingly, the self-trapped beam keeps moving toward the opposite direction as compared to the lateral shift of the peak intensity in the linear regime. Our further numerical calculations show that the *relatively stable* self-trapped states excited by the input beam shown in Fig. 2(a) occur when  $E_0$  falls into the range of  $0.2 \sim 0.4$ . In other words, when  $E_0$  is less than 0.2, the nonlinearity is too weak to balance the linear diffraction. While under a stronger  $E_0$ , the moving self-trapping states become unstable, breaking up rapidly during long-distance propagation. Moreover, the lateral shift of these self-localized nonlinear states gradually increases with the growing of  $E_0$  [see Fig. 2(g)]. We emphasize that the transverse momentum of such moving self-trapped states results from the balance between the asymmetric diffraction and the self-defocusing nonlinearity, and can be also considered as a type of symmetry-breaking behavior.

To demonstrate the aforementioned symmetry-breaking behavior, we use the experimental setup similar to that used in Refs. 2 and 9. An optically induced hexagonal photonic lattice (with  $13 \mu\text{m}$  lattice spacing) is created with an amplitude optical mask in a biased photorefractive SBN:60 crystal (1 cm long). Here, to observe the symmetry-breaking diffraction and nonlinear self-trapping state as shown in Fig. 2, we use a single Gaussian beam (with the wavelength 488 nm) tilted at the Bragg angle [with transverse wave vector  $\mathbf{k}_2$ , see the Fourier spectrum shown in the inset of Fig. 3(a)] to excite the Bloch mode at the  $M_1$  point.<sup>19</sup> We corroborate our experimental observations under single beam excitations by performing numerical simulations according to our experimental conditions. Figures 3(a) and 3(b) depict the linear (top) and nonlinear (bottom) numerical results, and the experimentally observed output beam patterns are displayed in Fig. 3(c). As we can see from the top panel of Fig. 3, in the absence of nonlinearity, the Bloch modes excited by the tilted input beam are mixed, i.e., they contain modes from different bands including the 2nd-band as the most pronounced one in addition to the 1st band.<sup>19</sup> Due to the mobility of the 2nd-band mode, the excited multivortex mode manifests itself from the cluster of the excited modes during propagation, and behaves asymmetric diffraction with the peak intensity position shifting toward the negative  $x$ -axis. Moreover, the 2nd-band mode does not behave obvious asymmetric diffraction, which might be suppressed by its mobility. After switching on the self-defocusing nonlinearity, the excited multivortex mode is indeed self-trapped but moves along the positive  $x$ -axis [see the bottom panel of Fig. 3]. In contrast, the 2nd-band mode diverges rapidly under the self-defocusing nonlinearity because of the normal diffraction. Due to the limited length of our crystal, the shifting of the self-trapping state is relatively small in our experiment, but large lateral displacement is obvious in

the simulation of long-distance propagation [Fig. 3(a)]. Our experimental results are in good agreement with the numerical results.

Now, we study the symmetry-breaking behaviors of elliptical optical beams in hexagonal photonic lattices. Figures 4(a)–4(d) depict the numerically calculated output intensity patterns by launching the Bloch modes at the  $M_1$  point with circular and elliptical truncations [see the insets for the inputs and power spectra]. Due to the threefold symmetry of the multivortex Bloch modes, the circular input beam with a sixfold symmetric intensity distribution will finally evolve into a triangular output intensity pattern [see Fig. 4(a)]. While for the input beams with elliptical envelopes, the inversion symmetry of the input beams will be broken after passing through the lattice structures [see Figs. 4(b)–4(d)]. These symmetry-breaking diffraction features can be explained with the diffraction curve. In Fig. 4(b), the Fourier spectrum of the input beam mainly concentrates at the  $\Gamma$ -M-X lines, resembling the case shown in Fig. 2(b). Therefore, the input beam exhibits the similar asymmetric diffraction as the stripe beam does. Likewise, the spectrum in Fig. 4(c) is mainly distributed along vertical direction at the M point, and the corresponding light components, respectively, refract to the bottom-left and top-left, representing a boomerang-shaped pattern. Note that the diffraction patterns in Figs. 4(b) and 4(c) exhibit mirror symmetry with respect to the  $x$ -axis. This is because the input elliptical beams and the Bloch waves at the  $M_1$  point possess the same mirror symmetry axis. However, when the symmetry axis of the input beam mismatches that of the Bloch wave, the symmetry will be totally broken, as shown in Fig. 4(d).

To experimentally demonstrate the symmetry-breaking behaviors of the two-dimensional multivortex beams, we keep our single beam excitation scheme. The tilted elliptical Gaussian beams with different orientations prepared by a pair of cylindrical lenses are launched into the lattice. Again, we perform numerical simulations according to the experimental conditions to corroborate our experimental observations. The numerical and experimental results are displayed in the top and bottom rows in Figs. 4(e)–4(g). It can be seen that after propagating a certain distance, the multivortex modes excited by the tilted elliptical beams manifest

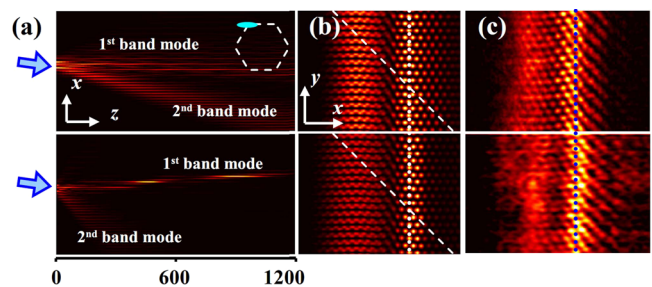


FIG. 3. (Color online) Numerical (a-b) and experimental (c) results of symmetry-breaking diffraction (top) and nonlinear self-trapping (bottom) excited by a tilted stripe Gaussian beam. (a) Side view of the beam propagation along  $z$ -direction for a section marked by the dashed line in (b), where the inset depicts the excitation condition. (b) Simulated output intensity patterns at  $z = 75$  (1 cm in experimental condition). (c) Experimentally observed output intensity patterns after passing through the 1 cm-long SBN crystal. The vertical dotted lines in (b) and (c) indicate the center of the input beam.

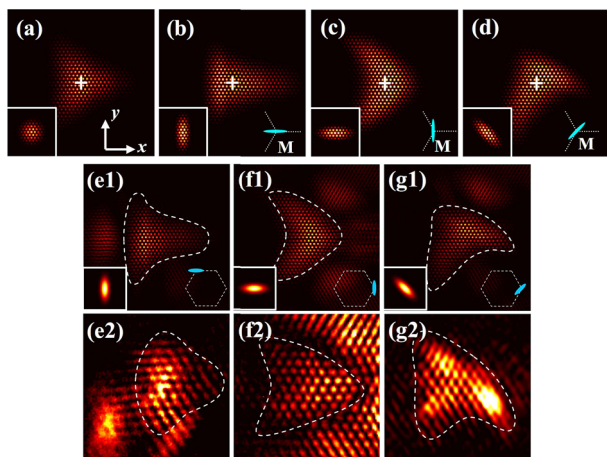


FIG. 4. (Color online) Numerical (a-d,e1-g1) and experimental (e2-g2) results of symmetry-breaking diffraction of elliptical multivortex beams in a hexagonal lattice. (a-d,e1-g1) display the output intensity patterns at  $z = 400$  (about 5.3 cm in experimental condition) with the centers of the input beam marked by the white crosses, where the insets show the input beams and the distribution of the power spectra at the M point; (e2-g2) show the corresponding experimental output light intensity patterns after propagation in a 2 cm-long SBN crystal.

themselves from the mixed Bloch modes, and the diffraction patterns [see the dashed curves in Figs. 4(e)–4(g)] coincide with that excited from the pure Bloch modes in Figs. 4(b)–4(d). From our numerical and experimental results, one can conclude that the symmetry of the diffraction pattern is governed by the input beam as well as the involved Bloch modes. Any mismatching between the symmetry axis of the input beams and that of the Bloch modes will lead to symmetry-breaking propagation. This will never happen in the lattices with orthogonal primitive axis. In addition, the above symmetry-breaking behaviors will be inverted for the Bloch mode at  $M_1'$  point [see Fig. 1(b)] due to the inversion symmetry between the M and  $M'$  points.

In summary, we have numerically and experimentally demonstrated the symmetry-breaking dynamics of Bloch modes at the high-symmetry M point of a hexagonal photonic lattice. We showed that such symmetry-breaking occurs when the input beam does not comply with the threefold-symmetry at the M point. In case of an input stripe beam, a moving self-

trapped state is formed in the presence of the self-defocusing nonlinearity. These results bring about an approach to control the flow of light with periodic photonic structures. We expect our findings could be extended to the wave dynamics in other period systems with similar symmetries, including BEC trapped in periodic optical potentials.

This work was supported by the Northwestern Polytechnical University (NPU) Foundation for Fundamental Research (JC200950), the Doctorate Foundation of NPU (CX200914), the 973 Program (2007CB613203 and 2012CB921900), the Program for Changjiang Scholars and Innovation Research Team, NSFC, AFOSR, and NSF.

<sup>1</sup>D. N. Christodoulides, F. Lederer, and Y. Silberberg, *Nature* **424**, 817 (2003).

<sup>2</sup>P. Zhang, C. Lou, S. Liu, J. Zhao, J. Xu, and Z. Chen, *Opt. Lett.* **35**, 892 (2010).

<sup>3</sup>C. R. Rosberg, D. N. Neshev, A. A. Sukhorukov, Y. S. Kivshar, and W. Krolikowski, *Opt. Lett.* **30**, 2293 (2005).

<sup>4</sup>R. Morandotti, H. S. Eisenberg, Y. Silberberg, M. Sorel, and J. S. Aitchison, *Phys. Rev. Lett.* **86**, 3296 (2001).

<sup>5</sup>J. W. Fleischer, M. Segev, N. K. Efremidis, and D. N. Christodoulides, *Nature* **422**, 147 (2003).

<sup>6</sup>P. Zhang, J. Zhao, F. Xiao, C. Lou, J. Xu, and Z. Chen, *Opt. Express* **16**, 3865 (2008).

<sup>7</sup>Y. Hu, C. Lou, S. Liu, P. Zhang, J. Yang, J. Xu, and Z. Chen, *Opt. Lett.* **34**, 1114 (2009).

<sup>8</sup>O. Bahat-Treidel, O. Peleg, and M. Segev, *Opt. Lett.* **33**, 2251 (2008).

<sup>9</sup>P. Zhang, S. Liu, C. Lou, F. Xiao, X. Wang, J. Zhao, J. Xu, and Z. Chen, *Phys. Rev. A* **81**, 041801(R) (2010).

<sup>10</sup>B. Terhalle, T. Richter, A. S. Desyatnikov, D. N. Neshev, W. Krolikowski, F. Kaiser, C. Denz, and Y. S. Kivshar, *Phys. Rev. Lett.* **101**, 013903 (2008).

<sup>11</sup>B. Terhalle, A. S. Desyatnikov, D. N. Neshev, W. Krolikowski, C. Denz, and Y. S. Kivshar, *Phys. Rev. Lett.* **106**, 083902 (2011).

<sup>12</sup>O. Peleg, G. Bartal, B. Freedman, O. Manela, M. Segev, and D. N. Christodoulides, *Phys. Rev. Lett.* **98**, 103901 (2007).

<sup>13</sup>Y. Kartashov, A. Szameit, V. Vysloukh, and L. Torner, *Opt. Lett.* **34**, 2906 (2009).

<sup>14</sup>O. Bahat-Treidel, O. Peleg, M. Segev, and H. Buljan, *Phys. Rev. A* **82**, 013830 (2010).

<sup>15</sup>M. Boguslawski, P. Rose, and C. Denz, *Appl. Phys. Lett.* **98**, 061111 (2011).

<sup>16</sup>P. Zhang, R. Egger, and Z. Chen, *Opt. Express* **17**, 13151 (2009).

<sup>17</sup>P. Zhang, N. K. Efremidis, A. Miller, Y. Hu, and Z. Chen, *Opt. Lett.* **35**, 3252 (2010).

<sup>18</sup>C. M. Anderson and K. P. Giapis, *Phys. Rev. Lett.* **77**, 2949 (1996).

<sup>19</sup>D. Mandelik, H. S. Eisenberg, Y. Silberberg, R. Morandotti, and J. S. Aitchison, *Phys. Rev. Lett.* **90**, 053902 (2003).